ACS Photonics

Letter

pubs.acs.org/journal/apchd5

Electric Field-Driven Shifting and Expansion of Photonic Band Gaps in 3D Liquid Photonic Crystals

Chun-Wei Chen,[‡] Cheng-Chang Li,[‡] Hung-Chang Jau, Lu-Chun Yu, Ching-Lang Hong, Duan-Yi Guo, Chun-Ta Wang, and Tsung-Hsien Lin*

Department of Photonics, National Sun Yat-Sen University, Kaohsiung 80424, Taiwan

Supporting Information

ABSTRACT: Highly tunable 3D liquid photonic crystals are demonstrated using low-dc-field-driven polymer-stabilized blue-phase liquid crystals. The central wavelength of the photonic band gap can be reversibly shifted to more than 200 nm away from the original position. Besides, by controlling the polymerization-induced morphology variations, the band gap can also be expanded from a bandwidth of around 30 nm to at least 310 nm, the first time a "white" blue phase is observed. Both types of band-gap modulation, namely, shifting and expansion, can be independently manipulated in any crystal axis without affecting the lattice spacings in the other dimensions. We envision polymer-stabilized blue-phase liquid crystals as a fascinating platform for photonic applications, such as 3D lasers, nonlinear optics, and photonic integrated circuits.

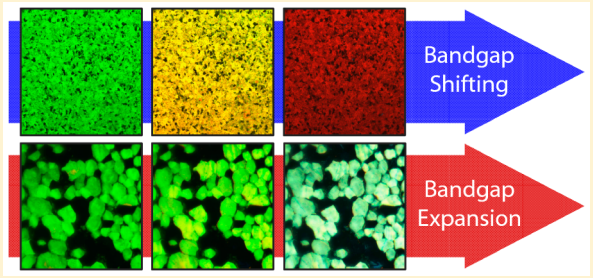

KEYWORDS: *photonic crystal, liquid crystal, blue phase, band-gap modulation*

Photonic crystals are optical materials with periodically distributed refractive indices.[1,2] Their photonic band-gap effect on the flow of photons makes them appear colored like the wings of a Morpho butterfly. They have potential for use in nanolasers, photovoltaics, nonlinear optics, and other applications. Given the rapid pace of development in photonic integrated circuits, three-dimensional (3D) photonic crystals are becoming increasingly important.[3−6] Common methods for fabricating 3D photonic crystals, such as photolithography or deposition, are not only costly but also time-consuming. The required precision and accuracy of such crystals considerably exceed those of 1D and 2D photonic crystals, to say nothing of having band gaps in the ultraviolet−visible spectrum and optical activity. Therefore, most current 3D photonic crystals are difficult to fabricate and only used at infrared or microwave wavelengths.

Blue-phase liquid crystals (BPLCs) with self-assembled 3D structure can be regarded as a liquid photonic crystal.[7] BPs are a class of particular mesophases of chiral nematics in which the director axes self-assemble into cylinders comprising double-twist helices. In order of emergence with increasing temperature, the phases are frequently designated as BPI, BPII, and BPIII. In the first two BPs, double-twist cylinders (DTCs) stack three-dimensionally throughout the bulk, forming a cubic crystal lattice. BPI is body-centered cubic (BCC) (Figure 1c), and BPII is simple cubic (SC). With a lattice spacing of a few hundred nanometers, the photonic band gaps (where light is forbidden) are in the visible spectrum. Satisfying Bragg's law, the reflection wavelength λ corresponding to the lattice plane (h k l) can be thus estimated by

$$\lambda = 2nd\cos\theta = \frac{2na\cos\theta}{\sqrt{h^2 + k^2 + l^2}} \quad (1)$$

where h, k, and l are the Miller indices, n is the average refractive index, d is the interplanar spacing of (h k l), a is the lattice constant, and θ is the angle between the light incidence and the crystallographic direction [h k l]. The chiral nature of BP causes the corresponding Bragg reflections to be circularly polarized. The handedness and mixing ratio of the chiral constituents can be controlled to determine the twist direction of the structure and the spectral position of the band gaps (from ultraviolet through visible to near-infrared). With respect to fabrication, the ability of spontaneous organization enables fast, simple, eco-friendly, cost-efficient, and high-precision fabrication of large photonic crystals.[8] BPLCs also feature topological defect structures that give rise to the 3D periodic confinement of nanoparticles, producing photonic crystalline metamaterials.[9] Due to its anisotropic liquid property, the uniqueness of BPLCs among photonic crystals lies in their ultrahigh tunability to external fields, including temperature,[10−12] light,[13] and electric fields.[14,15] Their photonic band gaps, crystal orientation, lattice structure, and birefringence can be readily modulated.

The innate topological structure (in which DTCs coexist with line defects) results in a narrow temperature range for the existence of BP of usually a few kelvins.[16] Numerous efforts have therefore been made to develop new BP materials that exist over an inherently wide range of temperature[12,17] and to

Received: June 4, 2015
Published: October 14, 2015

DOI: 10.1021/acsphotonics.5b00314
ACS Photonics 2015, 2, 1524−1531

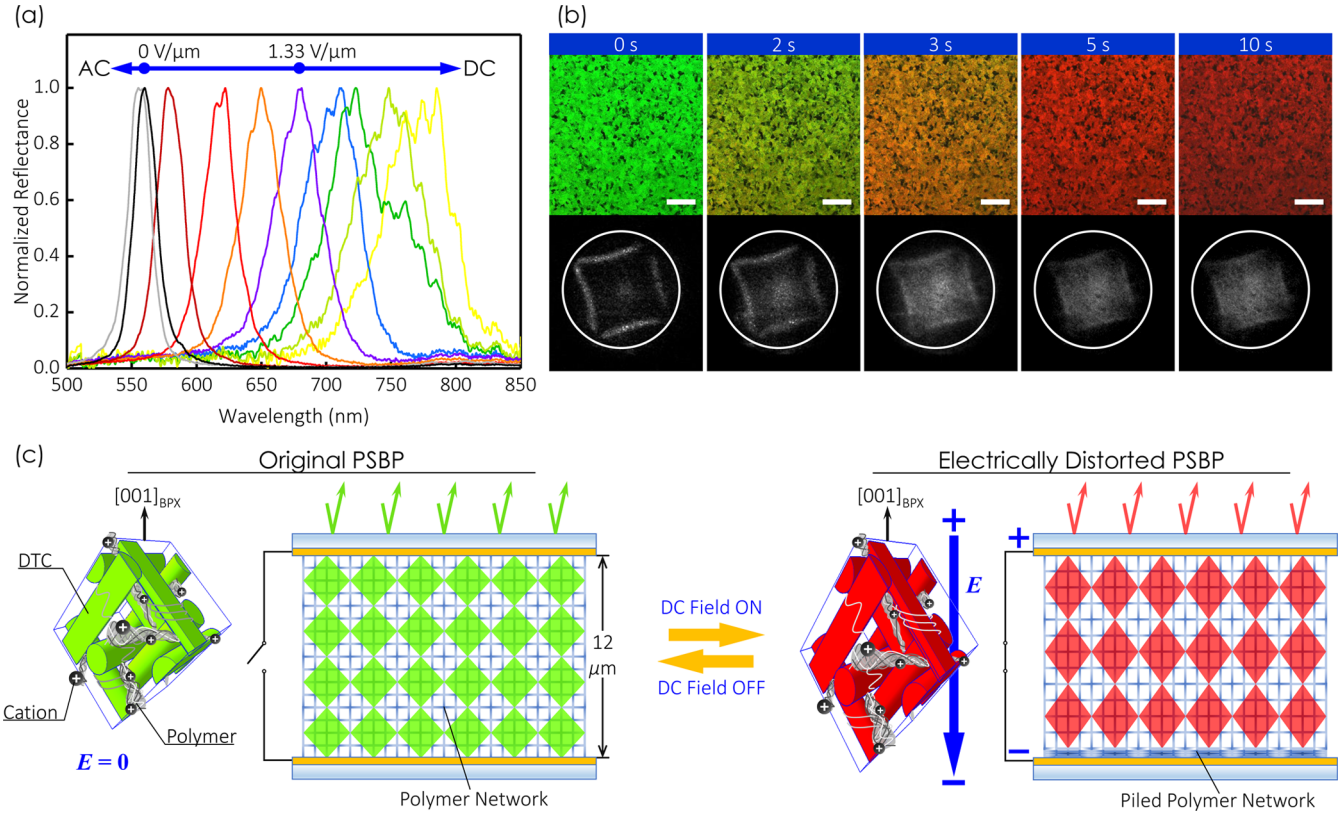

Figure 1. Red-shift of the photonic band gap: (a) normalized reflection spectra of a 12 μm thick PSBP film in various dc fields (0–2.67 V/μm) and an ac field (5.83 V/μm). See Figure S4a for the reflection spectra without normalization. (b) Time-resolved microscopic images (top, scale bars: 100 μm) and Kössel diagrams (bottom) captured under a dc field of 1.33 V/μm. The variation of Kössel pattern is more clearly presented in Video S3. (c) Schematics of the underlying mechanism for the dc-induced band-gap shifting in PSBP. The spectra were normalized to their peak intensities.

stabilize BPs using small amounts of solid impurities.[18,19] To date, the most successful strategy is that proposed by Kikuchi et al., who utilized an *in situ* generated polymer network to stabilize a BP lattice.[20] Polymer stabilization extended the BP temperature range from 1 K to more than 60 K, and the photonic band gaps became independent of temperature (cf. ref 21 and Figure S1), which are crucial for practical use. Unfortunately, polymer-stabilized (PS) BPs lost the high electric tunability of their photonic band gaps because the immobile polymer network governs the structure of its BP lattice.[22,23] Up until now, electrically switchable color reflections in PSBPs has been reported only by Lu and Chien.[24] However, an extensive but discontinuous shifting of photonic band gap was made due to the occurrence of electrostriction and phase transition from BPII to BPI; no expansion of the BP temperature range was observed after photopolymerization.

This work develops two novel electrically driven effects in a PSBP that can arbitrarily manipulate the photonic band gap of this liquid photonic crystal. The PSBP that consists of commercially available materials (Experimental Section) exhibits a temperature span of BP from 46 °C to at least 5 °C (the bottom limit of our temperature-controlled stage). Its electric tunability sets a new record in band-gap shifting. The latter effect—expansion of photonic band gaps—has never been observed in BPs or other 3D photonic crystals. The temporal behaviors during switching were recorded both visually and spectrally herein. The lattice distortion behavior was confirmed by examining Kössel diffractions, and the results thus obtained suggest the possibility of independent modulation of band gaps in each dimension.

Typical field-induced effects on BPs with and without a stabilizing polymer network are as follows. In a 1 kHz ac field of ~3.7 V/μm, the reflection band of the precursor in BPI (31.5 °C) underwent a red-shift of 22 nm (Figure S2), owing to lattice elongation along the field axis.[25] Reaching the stationary state took about 12 s. When the electric field was turned off, the reflection band relaxed at a similar speed, leveling off at a wavelength that was ~7 nm longer than the original. Tiribocchi et al. predicted the emergence of a metastable BP state based on the simulation result,[26] and this state has also been identified experimentally.[23] Switching to a dc field causes the BP crystallites to disorder quickly into a chiral nematic phase, as a consequence of electrohydrodynamic instabilities. Polymer stabilization can prevent structural change of the BP lattice. In this investigation, after the network was formed, not only was the thermal stability elevated, but also the effect of the electric field was restricted to local director reorientation. According to eq 1, a drop in effective index on the field axis shortens the reflection wavelength of a BP. Since the host material HTW114200-050 is dielectrically positive, the photonic band gap was reasonably blue-shifted (<5 nm) when a 1 kHz ac field was applied (Figure 1a). Local reorientation of directors also deformed the periodic index distribution, hence reducing the Bragg reflectivity.[22]

Applying a dc field across the 12 μm thick PSBP film gave rise to a strikingly different phenomenon. A fairly weak field of 1.33 V/μm moved the photonic band gap from 560 nm to 680 nm, turning the green film crimson, as shown in Figure 1.

DOI: 10.1021/acsphotonics.5b00314
ACS Photonics 2015, 2, 1524–1531

Raising the field to 2.67 V/μm, the band gap can be tuned as far as ~220 nm away from the original wavelength (Figure 1a). Figure 1b presents a series of microscopic images and corresponding Kössel diagrams (probing at 488 nm) that were captured during the red-shift process. The Kössel diffraction technique is a powerful tool to identify the structure and orientation of a photonic crystal with the lattice spacings on the order of a few hundred nanometers.[25,27−31] Instead of using X-ray for atom scale examination, the Kössel diagram can be obtained by visible light in the case of photonic crystals. On shining a single crystal with convergent monochromatic light that has a wavelength shorter than certain lattice spacing, some of the light is then diffracted from a set of lattice planes at an oblique angle, fulfilling Bragg's condition (cf. eq 1), forming cones of light. Rings and arcs (i.e., fragmented rings) of the diffracted light can provide clear evidence of the symmetry of the lattice structure. Given the Kössel pattern in Figure 1b, the PSBP crystal was found to possess 4-fold symmetry. Such a lattice structure arose from the field-induced lattice distortion of a [110]-oriented BPI crystal (cf. Figure S3) that occurred simultaneously with the electrical treatment for the PSBP precursor (Experimental Section) to make the (110) plane of most platelets face the same direction. References 32 and 33 suggest that the BP had experienced a phase transition and continuous deformation from the BCC BPI to the tetragonal BPX when the ac field was applied. The [110] pole of the deformed BCC crystal can be reindexed to [001] with respect to the coordinate system of the tetragonal lattice. The sample retained the [001]-oriented tetragonal lattice of BPX upon removal of the field. The series of Kössel diagrams also indicates that no phase transition occurred throughout the switching process. The weak scattering may be caused by the inhomogeneous distribution of the lattice spacing, indicating that the BP lattice was not perfectly distorted. Imperfect elongation of the lattice spacings also lowers the quality factor ($\lambda_0/\Delta\lambda$) of the photonic crystal (Figure S4b). Video S2 displays dynamics of the change in its macroscopic appearance. Figure S5 demonstrates that the red-shift was complete in ~10 s, and regaining the original color after the field was removed took ~20 s. The time constants are commensurate with the band-gap shifting in a polymer-stabilized cholesteric liquid crystal.[34,35] Since the response time varies negligibly with field strength (Figure S5), the response can be accelerated through overdriving. Besides, optimizing the recipe (e.g., constituents and mixing ratio of monomers) and polymerization conditions (e.g., exposure intensity and temperature) for the PSBP could also prove effective in improving the response time.

To gain insight into the anomalous behavior of the dc-biased PSBP, Figure 2 compares the variations of the reflection spectra that were measured from the positive-electrode and negative-electrode sides. Although the evolutions under the field were broadly similar, the relaxation processes differed substantially. The time-resolved reflection spectra from the positive-electrode side showed a comprehensible restoration of the distorted lattice: a continuous blue-shift (Figure 2a). However, the band at the negative side darkened within the first 2 s, after which a new peak appeared at ~535 nm before being red-shifted to the original wavelength (~560 nm) as the reflectance increased (Figure 2b). This evidence suggests that ionic interactions were responsible for the observed band-gap tuning. Generally, there are about 10^{13} ions per cm^3 in an LC mixture.[36] According to White et al., ester groups in polymers effectively trapped the

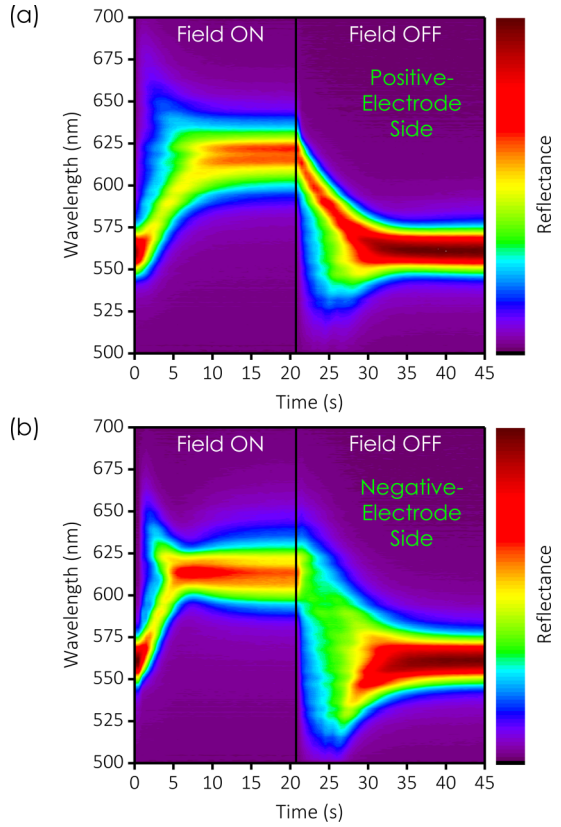

Figure 2. Dynamic responses of the reflection spectra detected from (a) the positive-electrode side and (b) the negative-electrode side of the 12 μm thick PSBP film.

positive ions, pulling the network toward the negative electrode when a dc field is applied.[37,38] With the aid of the orientational coupling of polymers with mesogens, the structural change in the BP lattice is enabled in a polymer-stabilized system. Each part of the polymer network experiences two forces that act in the same direction: (i) the attraction of the trapped cations by the negative electrode, i.e., electrophoresis, and (ii) the motion of fibrils that surround and are connected to the part of the polymer network. If the polymer is distributed uniformly throughout the thickness of the film, then almost every part of the network is displaced equally from its neighboring parts along the field axis, leading to a red-shift of the photonic band gap. However, the motion of the polymer fibrils is inhibited near the negative electrode because the thickness of the PSBP film is already fixed and predetermined when the rigid glass cell is fabricated. The polymer network piles up on this substrate, and a thin layer of shrunk photonic crystal lattice is thus formed, but the number of periods is too low to give rise to noticeable reflections. Upon removal of the field, the shrunk polymer network is unbound from the negative electrode and compresses the elongated part. Hence, the reflectance of the shrunk lattice is improved and the corresponding band gap is slowly red-shifted back to its original location, explaining the variations in Figure 2b. Concerning the elongated part of the electrically distorted lattice, the number of periods decreases with increasing field strength owing to the constant film thickness. This leads to a reduction in the reflectivity of the photonic crystal (Figure S4a). In addition, the orientational response of LC molecules to the electric field, i.e., local director reorientation, also exerts a negative impact on the photonic

DOI: 10.1021/acsphotonics.5b00314
ACS Photonics 2015, 2, 1524−1531

band-gap quality of the PSBP. Employing BP mixtures with small dielectric anisotropy could prevent the performance degradation of such liquid photonic crystals caused by field-induced director reorientation.

While color reflections only tell the change of lattice spacing along the field axis, Kössel diffractions disclose the influence of dc fields on the crystal structure in three dimensions. The four arcs shown in the Kössel diagram of a [001]-oriented BPX represent four oblique lattice planes, (1 1 1), (1−1 1), (−1 1 1), and (−1−1 1).[31] Under a dc bias, the Kössel arcs of the biased PSBP moved toward the center of the back focal plane (Figure 1b and Video S3); that is, the apex angles of the Kössel cones increased. To determine how the applied field influences the lattice spacings on the lateral axes, we made some in-plane-switching samples. Both samples with electrode spacings of 20 and 15 μm were examined. In Figure 3, the Kössel arcs on the left and right sides have the component of lattice spacing on the field axis (x-axis), while the upper and lower ones are only contributed by the spacings lying in the yz-plane (perpendicular to the field axis). On application of an in-plane dc field, the left and right arcs shifted inward, but there was no noticeable

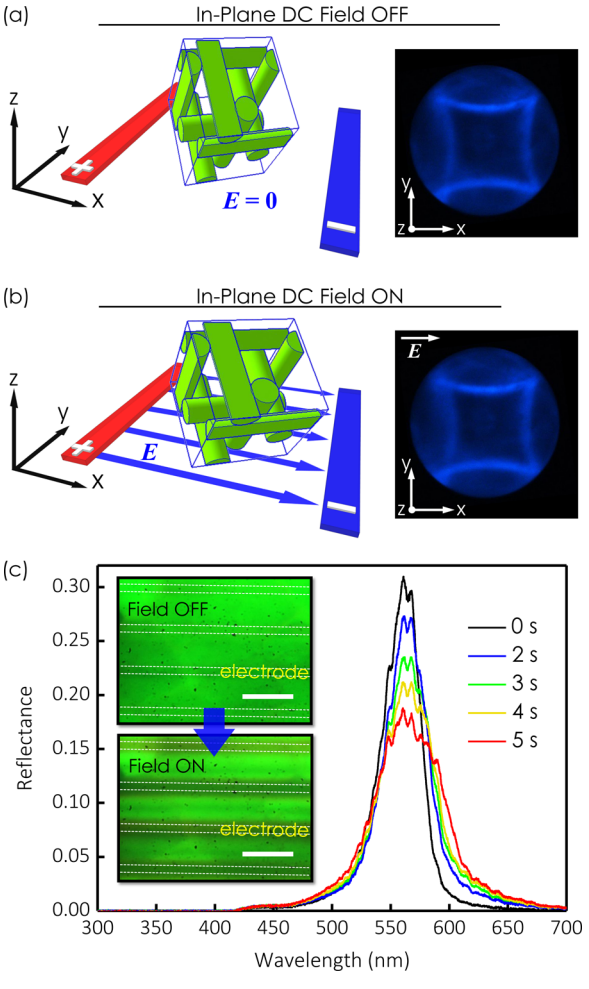

Figure 3. Modulation of the photonic crystal lattice under an in-plane electric field: Schematic depictions (left) and Kössel diagrams (right) of a $[001]_{BPX}$-oriented PSBP at (a) E_x = 0 V/μm and (b) E_x = 0.6 V/μm. (c) Time-resolved reflection spectra under a 1.6 V/μm in-plane field [inset: microscopic images taken before and after the in-plane field was switched on (scale bars: 20 μm)]. The change of Kössel pattern is more clearly presented in Video S4.

movement observed for the others (Figure 3a,b and Video S4). This implies that the extension of interplanar distance occurred only in the dimension that was parallel to the field axis, while the lateral spacings remained nearly constant instead of shrinking. In other words, the photonic band gaps in each dimension can be modulated independently of the others. To support our claim, the microscopic images and time-resolved reflection spectra under an in-plane field of 1.6 V/μm were recorded. Figure 3c reveals that the application of the in-plane field hardly shifted the normal reflection color and the corresponding photonic band gap, indicating that the PSBP retained its lattice spacing on the z-axis. Inevitably, in the electrode areas and their vicinity, the nonuniform electric field distribution slightly shifted the band gap toward longer wavelengths and degraded the overall reflectance. The reason the lattice spacings normal to the field axis were not electrically affected was that the lattice distortion originates from the field-induced deformation of the polymer network. Differing from the typical electrostriction of a pure BP, the firm polymer network prevented the LC molecules from reassembling along the directions perpendicular to the field axis to cancel the field-induced change in free energy. Through proper design of the electrode, such 3D photonic crystals allow independent control of photonic band gaps in each dimension, increasing their range of applications. It is noteworthy that the lattice elongation effect is not subject to $[001]_{BPX}$ // $\boldsymbol{E}$ but other crystal structures and orientations (e.g., $[001]_{BPI}$ in the Supporting Information). In brief, the PSBP used here has an extremely wide temperature range for the existence of BP (>40 K) and photonic band gaps insensitive to temperature; the proposed strategy enables continuous and large-scale band-gap tuning of more than 200 nm in a single BP, i.e., no inter-BP transitions involved. The proposed band-gap tuning is reversible and shows good repeatability, as indicated in Figure S7. Furthermore, the modulation of the band gap is along the dimension parallel to the field axis and is independent of the other two dimensions.

Changing the cell gap from 12 μm to 27 μm greatly altered the macroscopic distortion behavior of a dc-biased PSBP from band-gap shifting to expansion. As presented in Figure 4a, the 27 μm thick PSBP film turned from green to "white" under a dc field of 0.30 V/μm. The transmission spectrum (Figure 4c) demonstrates that the 34 nm wide notch melted toward both ends of the visible spectrum, becoming an extremely broad band from ~460 to 700 nm (wavelengths at half-maximum). Notably, the slopes at the band edges were quite small ($dT/d\lambda \approx 0.25\%$ per nm, where T denotes transmittance), so the expanded band gap still exhibited noticeable reflectivity at wavelengths below 460 nm and above 700 nm. The reduction in the notch depth upon band-gap expansion primarily arose from the finite film thickness that consists of various lattice spacings. The dark regions in Figure 4a are BP platelets reflecting only the ultraviolet light; that is, in such lattice orientations, their lowest order of Bragg diffractions along the viewing direction is in the ultraviolet spectrum. The reflection bands of these dark platelets also expand in dc fields. Upon band-gap broadening, some of them could reach the blue end of the visible spectrum, explaining why a few dark regions in Figure 4a turned slightly blue with very low brightness when a field of 0.30 V/μm was applied. The brightness was reasonably low because only a small portion of its reflections was in the visible range. Reflection spectra provide more information than transmission detection on the polarity of the field, owing to weak scattering from the polymer network and imperfect

DOI: 10.1021/acsphotonics.5b00314
ACS Photonics 2015, 2, 1524−1531

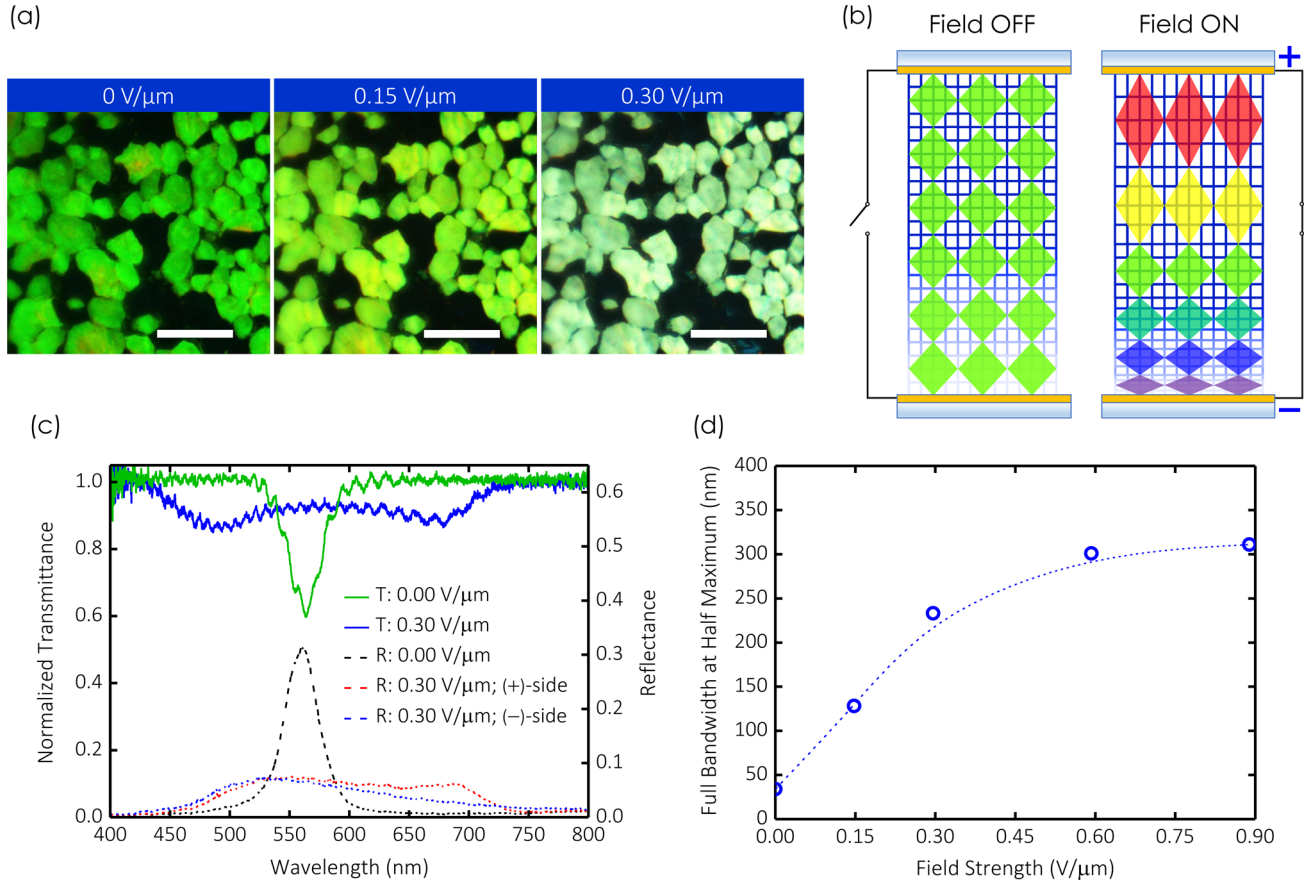

Figure 4. Expansion of photonic band gap. (a) Microscopic images of a 27 μm thick PSBP at various field strengths (scale bars: 100 μm). (b) Schematic depiction of the change in lattice spacing distribution when a field is applied. (c) Normalized transmission spectra and reflection spectra of the PSBP at 0 and 0.30 V/μm. (d) Bandwidths of the photonic band gap at various field strengths. The transmission spectra were normalized to the fitting curve shown in Figure S8.

distortion. While the PSBP on the positive-electrode side contributed more to the red part of the band, the reflection from the negative side peaked close to the blue edge, revealing that the network was elongated at the positive side and compressed at the negative side, supporting the ion-migration hypothesis.[31] Figure 4d compares the bandwidths at various field strengths, calculated from the reflection spectra. The band gap expanded to ~310 nm in a field of 0.89 V/μm, representing a 9-fold increase in bandwidth. The broadband reflectance can be improved through enlarging the cell gap.

Figure 5 plots the temporal responses of the transmission and reflection spectra of the band-gap expansion in a field of 0.30 V/μm. Both the switching (~50 s) and relaxation processes (~100 s) took about 5 times longer than for the 12 μm thick PSBP. The response time would have increased with the film thickness. The dynamics of lattice relaxation were similar to those in the shifting case. The positive side yielded a rising reflection peak that was blue-shifted from the red edge of the band, whereas the negative side yielded a retrieval from the blue edge. The difference between the spacing distributions of a distorted lattice in a 27 μm film and a 12 μm film is attributable to the distribution of polymer, as shown in Figure 4b. Ultraviolet light is well known to decay exponentially as it propagates through precursors, establishing a gradient of light intensity and a resultant diffusion of monomers. Monomer diffusion may not be easily identified in a thin 12 μm film, but may be strongly revealed by the consequent increase in the cell gap. As a result, the polymer network does not uniformly distribute regarding the density and thickness of polymer fibrils. This probably leads to inhomogeneous displacement of fibrils upon exposure to a dc field and resultant band-gap expansion, rather than shifting; however the underlying mechanism of this phenomenon awaits further study. Because the shifting and expansion of photonic band gaps both resulted from the ion-induced structural change in the polymer template of a BP lattice and just differed in polymer distribution throughout the film, there exists no exact cell gap between 12 and 27 μm that distinguishes the two effects. It is also believed that, through proper control of the ultraviolet-exposure/polymerization conditions (intensity, wavelength, etc.), selection of the resultant effect is possible and not subject to cell gap.

In summary, low dc fields (<3 V/μm) enabled the large-scale shifting and expansion of photonic band gaps in polymer-stabilized 3D liquid photonic crystals with a wide temperature range of BPX (>40 K). Direct current fields have a critical role in activating the motion of positively charged ions that are trapped in the polymer network, causing lattice distortion. In 12 μm thick films of PSBP, photonic band gaps were reversibly tuned within the widest spectral ranges yet achieved, exceeding 200 nm, with $[001]_{BPX}$ // E as well as $[001]_{BPI}$ // E. The corresponding Kössel diagrams suggest that the lattice spacings in various dimensions are independently controllable. To be specific, owing to the confinement of LC molecules in the immobile polymer network, only the lattice spacing along the

DOI: 10.1021/acsphotonics.5b00314
ACS Photonics 2015, 2, 1524−1531

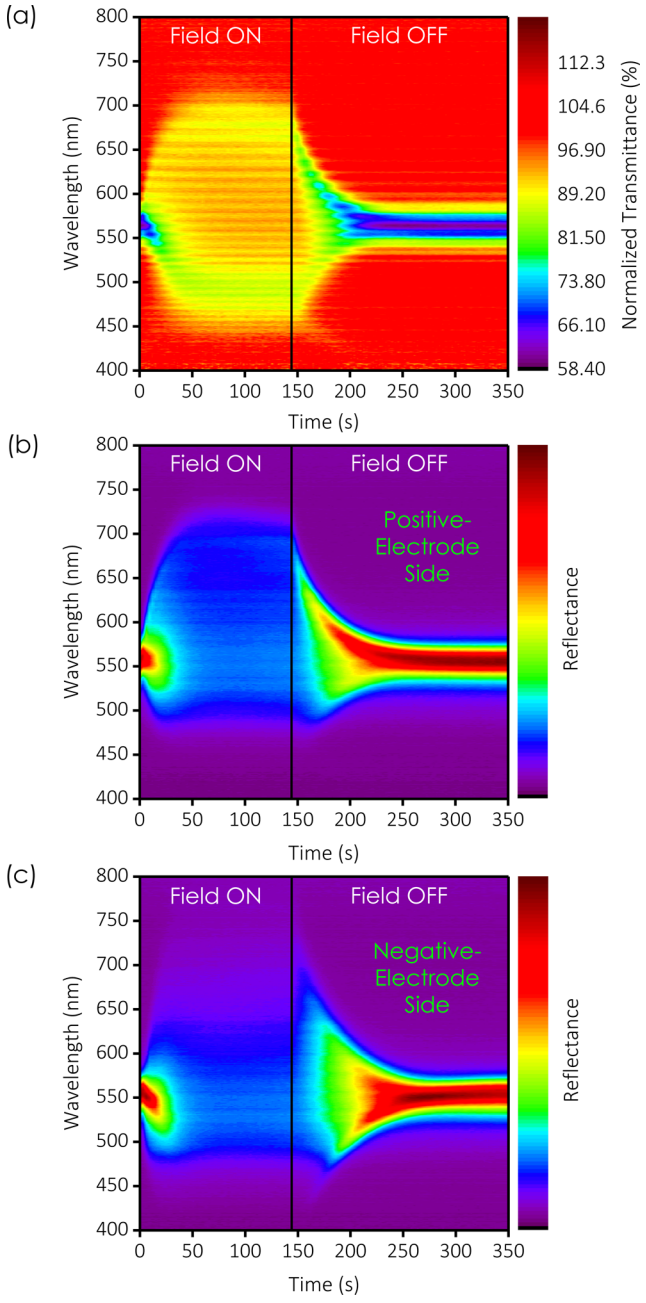

Figure 5. Dynamic responses of (a) the transmission spectra of the 27 μm thick PSBP as well as the reflection spectra detected from (b) the positive-electrode side and (c) the negative-electrode side.

field axis is modulated, whereas those in other dimensions stay the same, giving PSBPs an overwhelming advantage over pristine and nanoparticle/fibril-stabilized BPLCs. The application of a dc bias to a film with a larger thickness of 27 μm expanded the photonic band gaps, rather than shifting them. Applying a field of 0.89 V/μm electrically broadened the reflection band from a bandwidth of 34 nm to a width of 310 nm, encompassing almost the entire visible spectrum. These findings concerning high-tunability liquid 3D photonic crystals open a new window onto applied photonics.

EXPERIMENTAL SECTION

Two indium−tin-oxide (ITO)-coated glass slides without any surface treatment were separated by spacers (band-gap-shifting samples: 12 μm microspheres, Micropearl EX, Sekisui Chemical; band-gap-expansion samples: 27 μm plastic sheet) and bound with AB glue to form a sandwich cell allowing only vertical electric fields. The trielectrode cells allowing both vertical and in-plane switching were purchased from a local vendor. Some of the trielectrode cells have an in-plane electrode spacing of ∼15 μm, and the others are ∼20 μm; the cell gaps are all ∼16 μm. The PSBP precursor is formulated by homogeneously mixing 54.9 wt % nematic HTW114200-050 ($\Delta\varepsilon \approx 10.9$ at 1 kHz, 20 °C; $\Delta n \approx 0.222$ and $n_e \approx 1.729$ at 589 nm, 20 °C; purchased from HCCH), 36.6 wt % chiral smectic S811 (HCCH), 4 wt % mesogenic diacrylate RM257 (Merck), 4 wt % nonmesogenic acrylate EHA (Sigma-Aldrich), and 0.5 wt % photoinitiator Irgacure 651 (BASF). The phase sequence (cooling) of the precursor was ISO−36 °C−BPII−33 °C−BPI−28 °C−N*, where ISO and N* stand for the isotropic liquid phase and the cholesteric phase, respectively. The precursor was first heated to the isotropic phase (>36 °C) and then injected into the cell. Cooling the sample to 31.5 °C caused the precursor to form a polycrystalline BPI lattice. For the ease of investigation, a 1 kHz electric field of ∼3.33 V/μm was applied to induce lattice reorientation before conducting photopolymerization. Most of the crystallites thereby exhibit the same lattice plane perpendicular to the field axis. In our case, a phase transition to the tetragonal BPX occurred simultaneously. The sample was then exposed to ultraviolet light (XLite380, OPAS) with an intensity of 8 mW/cm^2 and peak wavelength at 368 nm for 30 min to ensure complete polymerization. During the cooling process, the PSBP underwent a phase transition from ISO to BPX at 46 °C, and the BPX was still stable when cooled to 5 °C, the bottom limit of our temperature-controlled stage (LTS 120, Linkam).

A function generator (33220A, Agilent) and a voltage amplifier (A400DI, FLC Electronics) were used to supply ac and dc fields. Reflection and transmission spectra were taken using the USB4000 spectrometer (Ocean Optics). Microscopic images and Kössel diagrams were captured using a charge-coupled device (DS-Fi1, Nikon) that was linked to a polarizing optical microscope (Eclipse LV100 POL, Nikon). In the Kössel diffraction examination, a 488 nm light with a bandwidth of 10 nm was employed as a light source. The Kössel rings can be observed in the back focal plane of the objective in a Bertrand-lens-inserted microscope.

ASSOCIATED CONTENT

Supporting Information

The Supporting Information is available free of charge on the ACS Publications website at DOI: 10.1021/acsphotonics.5b00314.

Temperature dependence of reflection wavelength of the PSBP, Kössel diagram of the precursor without electrical treatment ([110]-oriented BPI), reflection spectra in Figure 1a before normalization, quality factors ($\lambda_0/\Delta\lambda$) of the PSBP at various dc field strengths, field strength dependence and switching dynamics of reflection wavelengths of the precursor and PSBP, microscopic images and spectra of a $[001]_{BPI}$-oriented PSBP with and without a dc bias, repeatability test for dc switching, and fitting curve for normalization of the transmission spectra in Figure 4c (PDF)

Video of dynamics of the change in the photonic crystal's macroscopic appearance (AVI)

DOI: 10.1021/acsphotonics.5b00314
ACS Photonics 2015, 2, 1524−1531

Video of variation of Kössel pattern under a vertical dc field (AVI)

Video of change of Kössel pattern on application of an in-plane dc field (AVI)

AUTHOR INFORMATION

Corresponding Author

*E-mail: jameslin@faculty.nsysu.edu.tw.

Author Contributions

‡C.-W. Chen and C.-C. Li contributed equally.

Notes

The authors declare no competing financial interest.

ACKNOWLEDGMENTS

The authors gratefully acknowledge the Ministry of Science and Technology, Taiwan, for financially supporting this research under Contract No. 103-2112-M-110-012-MY3. The authors are indebted to Su-Chun Hsiao, Kun-Min Chang, Cheng-Yu Wang, Shuo Zhao, and Kai-Han Chang for inspiring discussions, and the reviewers for their constructive comments.

REFERENCES

(1) Yablonovitch, E. Inhibited Spontaneous Emission in Solid-State Physics and Electronics. *Phys. Rev. Lett.* **1987**, *58*, 2059−2062.

(2) John, S. Strong localization of photons in certain disordered dielectric superlattices. *Phys. Rev. Lett.* **1987**, *58*, 2486−2489.

(3) Rinne, S. A.; Garcia-Santamaria, F.; Braun, P. V. Embedded cavities and waveguides in three-dimensional silicon photonic crystals. *Nat. Photonics* **2008**, *2*, 52−56.

(4) von Freymann, G.; Ledermann, A.; Thiel, M.; Staude, I.; Essig, S.; Busch, K.; Wegener, M. Three-Dimensional Nanostructures for Photonics. *Adv. Funct. Mater.* **2010**, *20*, 1038−1052.

(5) Tandaechanurat, A.; Ishida, S.; Guimard, D.; Nomura, M.; Iwamoto, S.; Arakawa, Y. Lasing oscillation in a three-dimensional photonic crystal nanocavity with a complete bandgap. *Nat. Photonics* **2011**, *5*, 91−94.

(6) Turner, M. D.; Saba, M.; Zhang, Q.; Cumming, B. P.; Schroder-Turk, G. E.; Gu, M. Miniature chiral beamsplitter based on gyroid photonic crystals. *Nat. Photonics* **2013**, *7*, 801−805.

(7) Lin, T.-H.; Chen, C.-W.; Li, Q. Self-organized 3D Photonic Superstructure: Blue Phase Liquid Crystal. In *Anisotropic Nanomaterials: Preparation, Properties, and Applications*, Li, Q., Ed.; Springer: Heidelberg, 2015; pp 337−378.

(8) Castles, F.; Day, F. V.; Morris, S. M.; Ko, D. H.; Gardiner, D. J.; Qasim, M. M.; Nosheen, S.; Hands, P. J. W.; Choi, S. S.; Friend, R. H.; Coles, H. J. Blue-phase templated fabrication of three-dimensional nanostructures for photonic applications. *Nat. Mater.* **2012**, *11*, 599−603.

(9) Ravnik, M.; Alexander, G. P.; Yeomans, J. M.; Žumer, S. Three-dimensional colloidal crystals in liquid crystalline blue phases. *Proc. Natl. Acad. Sci. U. S. A.* **2011**, *108*, 5188−5192.

(10) Liu, H.-Y.; Wang, C.-T.; Hsu, C.-Y.; Lin, T.-H. Pinning effect on the photonic bandgaps of blue-phase liquid crystal. *Appl. Opt.* **2011**, *50*, 1606−1609.

(11) Chen, C.-W.; Jau, H.-C.; Lee, C.-H.; Li, C.-C.; Hou, C.-T.; Wu, C.-W.; Lin, T.-H.; Khoo, I. C. Temperature dependence of refractive index in blue phase liquid crystals. *Opt. Mater. Express* **2013**, *3*, 527−532.

(12) Hur, S.-T.; Lee, B. R.; Gim, M.-J.; Park, K.-W.; Song, M. H.; Choi, S.-W. Liquid-Crystalline Blue Phase Laser with Widely Tunable Wavelength. *Adv. Mater.* **2013**, *25*, 3002−3006.

(13) Lin, T.-H.; Li, Y.; Wang, C.-T.; Jau, H.-C.; Chen, C.-W.; Li, C.-C.; Bisoyi, H. K.; Bunning, T. J.; Li, Q. Red, Green and Blue Reflections Enabled in an Optically Tunable Self-Organized 3D Cubic Nanostructured Thin Film. *Adv. Mater.* **2013**, *25*, 5050−5054.

(14) Kitzerow, H. S. The Effect of Electric Fields on Blue Phases. *Mol. Cryst. Liq. Cryst.* **1991**, *202*, 51−83.

(15) Wang, C.-T.; Liu, H.-Y.; Cheng, H.-H.; Lin, T.-H. Bistable effect in the liquid crystal blue phase. *Appl. Phys. Lett.* **2010**, *96*, 041106.

(16) Meiboom, S.; Sethna, J. P.; Anderson, P. W.; Brinkman, W. F. Theory of the Blue Phase of Cholesteric Liquid Crystals. *Phys. Rev. Lett.* **1981**, *46*, 1216−1219.

(17) Coles, H. J.; Pivnenko, M. N. Liquid crystal 'blue phases' with a wide temperature range. *Nature* **2005**, *436*, 997−1000.

(18) Yoshida, H.; Tanaka, Y.; Kawamoto, K.; Kubo, H.; Tsuda, T.; Fujii, A.; Kuwabata, S.; Kikuchi, H.; Ozaki, M. Nanoparticle-Stabilized Cholesteric Blue Phases. *Appl. Phys. Express* **2009**, *2*, 121501.

(19) Yabu, S.; Tanaka, Y.; Tagashira, K.; Yoshida, H.; Fujii, A.; Kikuchi, H.; Ozaki, M. Polarization-independent refractive index tuning using gold nanoparticle-stabilized blue phase liquid crystals. *Opt. Lett.* **2011**, *36*, 3578−3580.

(20) Kikuchi, H.; Yokota, M.; Hisakado, Y.; Yang, H.; Kajiyama, T. Polymer-stabilized liquid crystal blue phases. *Nat. Mater.* **2002**, *1*, 64−68.

(21) Yokoyama, S.; Mashiko, S.; Kikuchi, H.; Uchida, K.; Nagamura, T. Laser Emission from a Polymer-Stabilized Liquid-Crystalline Blue Phase. *Adv. Mater.* **2006**, *18*, 48−51.

(22) Chen, Y.; Wu, S.-T. Electric field-induced monodomain blue phase liquid crystals. *Appl. Phys. Lett.* **2013**, *102*, 171110.

(23) Yoshida, H.; Yabu, S.; Tone, H.; Kawata, Y.; Kikuchi, H.; Ozaki, M. Secondary electro-optic effect in liquid crystalline cholesteric blue phases. *Opt. Mater. Express* **2014**, *4*, 960−968.

(24) Lu, S.-Y.; Chien, L.-C. Electrically switched color with polymer-stabilized blue-phase liquid crystals. *Opt. Lett.* **2010**, *35*, 562−564.

(25) Heppke, G.; Jérôme, B.; Kitzerow, H.-S.; Pieranski, P. Electrostriction of the cholesteric blue phases BPI and BPII in mixtures with positive dielectric anisotropy. *J. Phys. (Paris)* **1989**, *50*, 2991−2998.

(26) Tiribocchi, A.; Gonnella, G.; Marenduzzo, D.; Orlandini, E. Switching dynamics in cholesteric blue phases. *Soft Matter* **2011**, *7*, 3295−3306.

(27) Pieranski, P.; Dubois-Violette, E.; Rothen, F.; Strzelecki, L. Geometry of Kossel lines in colloidal crystals. *J. Phys. (Paris)* **1981**, *42*, 53−60.

(28) Cladis, P. E.; Garel, T.; Pieranski, P. Kossel Diagrams Show Electric-Field-Induced Cubic-Tetragonal Structural Transition in Frustrated Liquid-Crystal Blue Phases. *Phys. Rev. Lett.* **1986**, *57*, 2841−2844.

(29) Jérôme, B.; Pieranski, P.; Godec, V.; Haran, G.; Germain, C. Determination of the blue phase II structure. *J. Phys. (Paris)* **1988**, *49*, 837−844.

(30) Heppke, G.; Jerome, B.; Kitzerow, H. S.; Pieranski, P. Electrostriction of BPI and BPII for blue phase systems with negative dielectric anisotropy. *J. Phys. (Paris)* **1989**, *50*, 549−562.

(31) Miller, R. J.; Gleeson, H. F. Lattice Parameter Measurements from the Kossel Diagrams of the Cubic Liquid Crystal Blue Phases. *J. Phys. II* **1996**, *6*, 909−922.

(32) Pieranski, P.; Cladis, P. E. Field-induced tetragonal blue phase (BP X). *Phys. Rev. A: At., Mol., Opt. Phys.* **1987**, *35*, 355−364.

(33) Yoshida, H.; Yabu, S.; Tone, H.; Kikuchi, H.; Ozaki, M. Electro-Optics of Cubic and Tetragonal Blue Phase Liquid Crystals Investigated by Two-Beam Interference Microscopy. *Appl. Phys. Express* **2013**, *6*, 062603.

(34) McConney, M. E.; Tondiglia, V. P.; Natarajan, L. V.; Lee, K. M.; White, T. J.; Bunning, T. J. Electrically Induced Color Changes in Polymer-Stabilized Cholesteric Liquid Crystals. *Adv. Opt. Mater.* **2013**, *1*, 417−421.

(35) Lee, K. M.; Tondiglia, V. P.; McConney, M. E.; Natarajan, L. V.; Bunning, T. J.; White, T. J. Color-Tunable Mirrors Based on Electrically Regulated Bandwidth Broadening in Polymer-Stabilized Cholesteric Liquid Crystals. *ACS Photonics* **2014**, *1*, 1033−1041.

(36) Wu, P.-C.; Hou, C.-T.; Hsiao, Y.-C.; Lee, W. Influence of methyl red as a dopant on the electrical properties and device performance of liquid crystals. *Opt. Express* **2014**, *22*, 31347−31355.

DOI: 10.1021/acsphotonics.5b00314
ACS Photonics 2015, 2, 1524−1531

(37) Tondiglia, V. P.; Natarajan, L. V.; Bailey, C. A.; McConney, M. E.; Lee, K. M.; Bunning, T. J.; Zola, R.; Nemati, H.; Yang, D.-K.; White, T. J. Bandwidth broadening induced by ionic interactions in polymer stabilized cholesteric liquid crystals. *Opt. Mater. Express* **2014**, *4*, 1465−1472.
(38) Nemati, H.; Liu, S.; Zola, R. S.; Tondiglia, V. P.; Lee, K. M.; White, T.; Bunning, T.; Yang, D.-K. Mechanism of electrically induced photonic band gap broadening in polymer stabilized cholesteric liquid crystals with negative dielectric anisotropies. *Soft Matter* **2015**, *11*, 1208−1213.

DOI: 10.1021/acsphotonics.5b00314
ACS Photonics 2015, 2, 1524−1531